 CMES, vol.7, no.2, pp.223-232, 2005

Method of Fundamental Solutions for Scattering Problems of Electromagnetic Waves

D.L. Young[1,2] **and J.W. Ruan**[2]

Abstract: The applications of the method of fundamental solutions (MFS) for modeling the scattering of time-harmonic electromagnetic fields, which are governed by vector Helmholtz equations with coupled boundary conditions, are described. Various perfectly electric conductors are considered as the scatterers to investigate the accuracy of the numerical performance of the proposed procedure by comparing with the available analytical solutions. It is also the intention of this study to reveal the characteristics of the algorithms by comparisons with other numerical methods. The model is first validated to the exact solutions of the electromagnetic wave propagation problems for the scatterers of a circular cylinder and a sphere. The radar cross sections (RCS) of a prolate spheroid are then presented to illustrate the predictive capability of the algorithms for more complex geometric shapes of the scatterers. The present investigation has demonstrated that the MFS technique is simple, efficient, and accurate for modeling 2D and 3D electromagnetic scattering problems.

keyword: electromagnetic scattering, method of fundamental solutions, radar cross section, time-harmonic, scatterer of a circular cylinder, scatterer of a sphere, scatterer of a spheroid

1 Introduction

The meshless or meshfree numerical methods have become popular trends in scientific computing. In general classification there are two categories, namely the domain-type and boundary-type. Some former examples are the meshless finite volume method (Atluri, Han and Rajendran, 2004) and the meshless finite element method (Atluri and Shen, 2002).The typical examples for latter are the meshless boundary element method and the method of fundamental solutions. The method of fundamental solutions (MFS), a kind of boundary-type meshless numerical method, adopted in this paper is claimed as a special Trefftz method (Trefftz, 1926; Cho et al, 2004). The concept of the MFS is to decompose the solution of partial differential equations (PDEs) by the superposition of the fundamental functions. The singular fundamental solutions are the responding equations due to concentrated sources, with appropriate intensities of the singularities. The intensities are in fact the unknown expansion coefficients to be determined when the MFS is used. The magnitudes and locations of the sources of the singularities can be obtained from the approximate satisfaction of a certain number of boundary conditions by the method of the collocation. Therefore the MFS is somewhat analogous to the indirect boundary integral equation method (BIEM). However MFS not only inherits the advantages of the unbounded region and significantly reduced mesh generation of the BIEM, but also has some unique advantages. For examples, the MFS avoids singular kernels problems by addressing the singularities of the fundamental solutions on a fictitious boundary outside the study domain. In the mean time the simple implementation of the governing equations without the integration of the boundary points can be easily achieved. Furthermore, there is no need to establish the mesh connectivity in the physical boundary and domain. Only the boundary discretization is required to determine the intensities of the singularities for the fundamental solutions as compared with the conventional numerical schemes or meshless local Petrov-Galerkin (MLPG) methods (Atluri, 2004).

The MFS is attributed to Kupradze and Aleksidze (1964) in a paper published in Russian, and the utility of the MFS technique was later introduced into computational communities by Mathon and Johnston (1977). In concept, the MFS is similar to the boundary knot method (BKM) [Chen (2002A); Chen & Tanaka (2002)] and the boundary particle method (BPM) [Chen (2002B)] except

[1] Corresponding author, Fax: +886-2-23626114,
Email: dlyoung@ntu.edu.tw.
[2] Department of Civil Engineering & Hydrotech Research Institute, National Taiwan University, Taipei, 10617, TAIWAN.

the singularity and the symmetric properties of resulted system matrix. Recently, Golberg (1995) and Golberg & Chen (1997) combined the dual reciprocity method (DRM) with the MFS as a meshless numerical method to deal with the Poisson's equation. Fairweather and Karageorghis (1998) also provided an excellent review about the MFS for elliptic boundary value problems. Chen, Golberg and Rashed (1998) on the other hand utilized the DRM-MFS to solve the diffusion equation. Tsai, Young and Cheng (2002) further employed the DRM-MFS to solve the 3D Stokes flows. Other researches involving the MFS solutions of fluids and elastic solids were cited by Fairweather, Karageorghis and Martin, (2003), which surveyed the MFS applications in scattering and radiation problems. As far as the computational electromagnetics is concerned [Chew,Song,Cui,Velamparambil,Hastriter and Hu (2004); Reitich and Tamma (2004)], Jingguo, Ahmed and Lavers (1990) utilized the MFS to analyze the eddy current problems. However, the MFS modeling of electromagnetic scattering problems remains hot research topics. In this study, we will first use the MFS to deal with this kind of problems with simple shape of scatterers, thus the analytic solutions (Harrington, 1961) are available to compare with our MFS numerical results. A variety of numerical techniques to investigate the same electromagnetic scattering problems was also undertaken. We will compare the MFS results with different numerical approaches to evaluate their comparative merits and demerits. For example, Chen (2002) has used the conventional boundary element method (BEM) to simulate the two-dimensional and three-dimensional simple electromagnetic scattering problems. Chiu and Young (2003) on the other hand employed the non-singular boundary integral equation (NSBIE) method to study the same problems. In addition, the three-dimensional perfectly electric conducting sphere studied by Morgan, Brookes, Hassan and Weatherill (1998) and the two-dimensional perfectly electric conducting circular cylinder by Ledger, Morgan, Hassan and Weatherill (2002), both using the finite element method (FEM), are all taken into account to compare the characteristics of these numerical methods. Furthermore, to extend to some more complex spheroidal geometry, such as a prolate spheroid, the RCS, to be defined later, and the contour of scattered components are finally computed in this study to illustrate the predictive power of the MFS for the complex scatterer. For more complicate 3D electromagnetic scattering simulations the work of Hassan, Morgan, Jones, Larwood and Weatherill is referred.

2 Electromagnetic Preliminary

2.1 Governing Equations and Boundary Conditions

The Maxwell's equations which govern the electromagnetic wave propagation are reduced to the wave equations by raising the orders to result in the uncoupled second-order partial differential equations. Since the electromagnetic wave propagating through the free space will be discussed, the assumption of the lossless source-free medium reduces the Maxwell's equations to the simplest vector Helmholtz forms, expressed as

$$\nabla^2 \overrightarrow{E} = \mu\varepsilon \frac{\partial^2 \overrightarrow{E}}{\partial t^2}. \tag{1}$$

$$\nabla^2 \overrightarrow{H} = \mu\varepsilon \frac{\partial^2 \overrightarrow{H}}{\partial t^2}. \tag{2}$$

The general behavior of a wave as a function of time can always be expressed as a superposition of waves at different frequencies. Thus, we assume time-harmonic for both the electric and magnetic waves:

$$\overrightarrow{E} = Re\left(\overrightarrow{E_0} e^{i\omega t}\right). \tag{3}$$

$$\overrightarrow{H} = Re\left(\overrightarrow{H_0} e^{i\omega t}\right). \tag{4}$$

where $e^{i\omega t}$ denotes the time variation of the wave forms for these time-harmonic fields, whilst the superscript ω is the angular frequency of the wave. Both phasor fields of $\overrightarrow{E}_0$ and $\overrightarrow{H}_0$ are the functions of position only, and are in general the complex-valued functions. Substituting Eq. 3 into Eq. 1 and Eq. 4 into Eq. 2 respectively, the homogeneous vector Helmholtz equations, which are the main governing equations throughout this paper, are obtained in the following forms.

$$\nabla^2 \overrightarrow{E} + \mu\varepsilon\omega^2 \overrightarrow{E} = \nabla^2 \overrightarrow{E} + k^2 \overrightarrow{E} = 0. \tag{5}$$

$$\nabla^2 \overrightarrow{H} + \mu\varepsilon\omega^2 \overrightarrow{H} = \nabla^2 \overrightarrow{H} + k^2 \overrightarrow{H} = 0. \tag{6}$$

where the subscript 0 for the phasor has been omitted whenever no confusion is expected to arise, and the k represents the wavenumber, which is determined by the following formula

$$k = \omega\sqrt{\mu\varepsilon} = \frac{\omega}{1/\sqrt{\mu\varepsilon}} = \frac{\omega}{c} = \frac{2\pi}{\lambda}. \tag{7}$$

where λ is the wavelength and c is the wave velocity. The total electric and magnetic fields, regarded as being combined with both the incident and scattered components can be expressed in these forms.

$$\overrightarrow{E}^t = \overrightarrow{E}^i + \overrightarrow{E}^s. \tag{8}$$

$$\overrightarrow{H}^t = \overrightarrow{H}^i + \overrightarrow{H}^s. \tag{9}$$

where $\overrightarrow{E}^t, \overrightarrow{H}^t$ represent the total electric and magnetic fields in the presence of an obstacle, respectively. And $\overrightarrow{E}^i, \overrightarrow{H}^i$ represent the electric and magnetic fields in the absence of the obstacle. They are called the incident fields. The fields $\overrightarrow{E}^s, \overrightarrow{H}^s$ represent the perturbation fields of the total electric and magnetic fields in the presence of the obstacle, they are usually referred to as the scattered fields. The scattered fields are therefore can be expressed by the following governing equations.

$$\nabla^2 \overrightarrow{E}^s + k^2 \overrightarrow{E}^s = 0. \tag{10}$$

$$\nabla^2 \overrightarrow{H}^s + k^2 \overrightarrow{H}^s = 0. \tag{11}$$

After addressing the governing equations, we discuss about the boundary conditions in the following. The region outside the perfectly electric conductor is the main concerned domain of interest. Applying the integral form of the Maxwell's equations to a small region, we obtain the tangential component of the total electric fields and the normal component of the total magnetic fields. Both fields must vanish on the boundary of a perfectly electrical conductor, i.e.

$$\overrightarrow{n} \times \overrightarrow{E}^s = -\overrightarrow{n} \times \overrightarrow{E}^i. \tag{12}$$

$$\overrightarrow{n} \cdot \overrightarrow{H}^s = -\overrightarrow{n} \cdot \overrightarrow{H}^i. \tag{13}$$

where $\overrightarrow{n}$ denotes the unit outward normal vector to the surface of the conductor.

2.2 Radar Cross Section

The radar cross section (RCS), an essential parameter in the radar system and electronic warfare system, reveals the scattered field characteristic of the target. It is closely related to the shape and the material of the target; and the angle, frequency and polarization of the transmitter; as well as the polarization of the receiver. The RCS is employed to examine the accuracy of the present numerical model. Moreover the verified model is used to compute the RCS of other shapes. The definition of the RCS, "the area intercepting the amount of power that, when scattered isotropically, produces at the receiver a density that is equal to the density scattered by the actual target", can be found in Balanis (1982). The RCS is referred to as the scattering width (SW), the unit is the length for a two-dimensional target, whereas the unit of the RCS for a three-dimensional target is the area. Hence the equation forms of the two-dimensional target and three-dimensional target are written as below, respectively.

$$\sigma_{2-D} = \begin{cases} \lim\limits_{\rho\to\infty} \left[2\pi\rho \dfrac{\left|\overrightarrow{E}^s\right|^2}{\left|\overrightarrow{E}^i\right|^2} \right] \\ \lim\limits_{\rho\to\infty} \left[2\pi\rho \dfrac{\left|\overrightarrow{H}^s\right|^2}{\left|\overrightarrow{H}^i\right|^2} \right] \end{cases}. \tag{14}$$

$$\sigma_{3-D} = \begin{cases} \lim\limits_{r\to\infty} \left[4\pi r^2 \dfrac{\left|\overrightarrow{E}^s\right|^2}{\left|\overrightarrow{E}^i\right|^2} \right] \\ \lim\limits_{r\to\infty} \left[4\pi r^2 \dfrac{\left|\overrightarrow{H}^s\right|^2}{\left|\overrightarrow{H}^i\right|^2} \right] \end{cases}. \tag{15}$$

where ρ, r are the distances from the target to the observation point in 2D and 3D respectively, $\overrightarrow{E}^s, \overrightarrow{E}^i$ are scattered, and incident electric fields, and $\overrightarrow{H}^s, \overrightarrow{H}^i$ are scattered, and incident magnetic fields, respectively.

3 Numerical Algorithm

The basic idea of the MFS is to solve differential equations by making use of the fundamental solutions to the problem. This method makes use of the fundamental solutions of the problem by satisfying the governing equations in the interested domain. Since the fundamental solutions may not satisfy any particular set of boundary conditions, the fundamental solutions are appropriately scaled by a number of unknown coefficients. These coefficients can be determined from the approximate satisfaction of the boundary conditions by the method of collocation.

For the Helmholtz equations of Eq. 10 and Eq. 11, we may assume that the required solution is a linear combination of the fundamental solutions of the Helmholtz operator, i.e.

$$\Phi(x_i) = \sum_{j=1}^{M} \beta_j g(R_{ij}). \tag{16}$$

where

$$g(R_{ij}) = \begin{cases} -\frac{1}{4}Y_0(kR_{ij}) - i\frac{1}{4}J_0(kR_{ij}) \text{ for 2D} \\ \dfrac{\cos(kR_{ij})}{4\pi R_{ij}} - i\dfrac{\sin(kR_{ij})}{4\pi R_{ij}} \text{ for 3D} \end{cases} . \quad (17)$$

are the fundamental solutions of the Helmholtz operator, and R_{ij} is the distance between the boundary point x_i and the j-th source point x_j, which is located outside the physical domain, and M is the number of source nodes. Wherein, $J_0()$ and $Y_0()$ are the Bessel functions of the first and second kinds of order zero. Furthermore, the derivative of the fundamental solutions in Eq. 16 and 17 are obtained through

$$\frac{\partial \Phi(x_i)}{\partial n_i} = \sum_{j=1}^{M} \beta_j \frac{\partial g(R_{ij})}{\partial n_i}. \quad (18)$$

After evaluating β_j's through collocating at the boundary and source points, we get the required solutions through the Eq. 16 and 17. If, the problem we are concerned, is, in, the spherical, coordinates, or in the cylindrical coordinates, the differential term in Eq. 18 can be further written as:

$$\frac{\partial g(R_{ij})}{\partial n_i} = \frac{\partial g(R_{ij})}{\partial (R_{ij})} \frac{\partial (R_{ij})}{\partial n_i}$$

$$= \begin{cases} \left(\frac{\vec{R_{ij}} \bullet \vec{n_i}}{4R_{ij}} k\right) [Y_1(kR_{ij}) + iJ_1(kR_{ij})] \text{ for 2D} \\ \left(\frac{\vec{R_{ij}} \bullet \vec{n_i}}{R_{ij}}\right) \frac{-e^{-ikR_{ij}}}{4\pi R_{ij}^2} (ikR_{ij} + 1) \text{ for 3D} \end{cases} \quad (19)$$

For more general discussions and reviews about the MFS for scattering and radiation problems, the reference of Fairweather, Karageorghis and Martin (2003) is suggested.

4 Numerical Examples

4.1 Scattering By A Conducting Circular Cylinder

Let us consider a transverse electric (TE^z) and a transverse magnetic (TM^z) field of uniform plane wave with unit amplitude travels along the direction of the positive x axis. The TE^z and TM^zwaves are normally incident upon a perfectly conducting circular cylinder of radius a, in the source-free and lossless space as shown in Fig. 1 (a) and (b) respectively. Due to the simplicity of the normally incident wave, the problem can be reduced from a 3-D problem to a 2-D one. Finally, to normalize the problem, the permittivity, permeability and wave length will be treated as follows

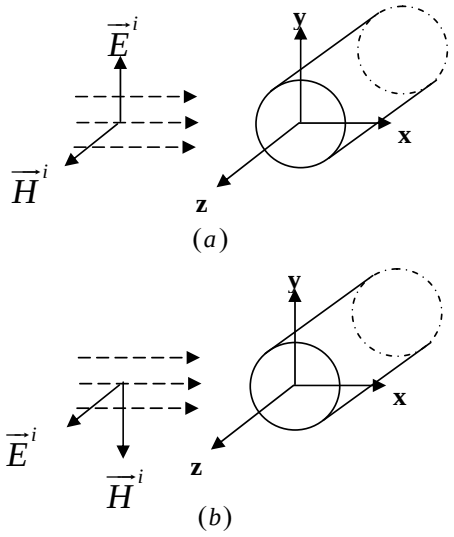

Figure 1 : Normally incident plane wave of: (a) TE^z (b) TM^z wave on a perfectly conducting circular cylinder.

$$\mu = \varepsilon = 1 \quad \text{and} \quad \lambda = 1 \quad (20)$$

Therefore, the wavenumber and angular frequency are determined from Eq. 7. To validate the MFS technique, first of all, the real part of the computed scattered electric field (E_z^s) along $r = 4$ of a plane TM^z wave by radius $a = 2$ perfectly conducting circular cylinder is displayed in Fig. 2. The numerical simulation of the scattered electric field is compared with the results of analytical solution [Harrington (1961)] and the conventional BEM [Chen (2002)] as well as the NSBIE [Chiu and Young (2003)] methods, as depicted in Fig. 2. The comparison with analytic solutions confirms very accurate results of the MFS, and the comparisons with the conventional BEM and the NSBIE methods also reveal good results for all the numerical simulations.Furthermore, the computed data are summarized in Tab. 1 to analyze the CPU time for these methods. It can be observed that the CPU time for the MFS calculation is much lesser than the conventional BEM, and the NSBIE method. The outstanding saving in the CPU time is a very important asset of the MFS which, unlike the BEM and the NSBIE methods, the boundary integration procedure in generating discretization matrix of the governing equation is

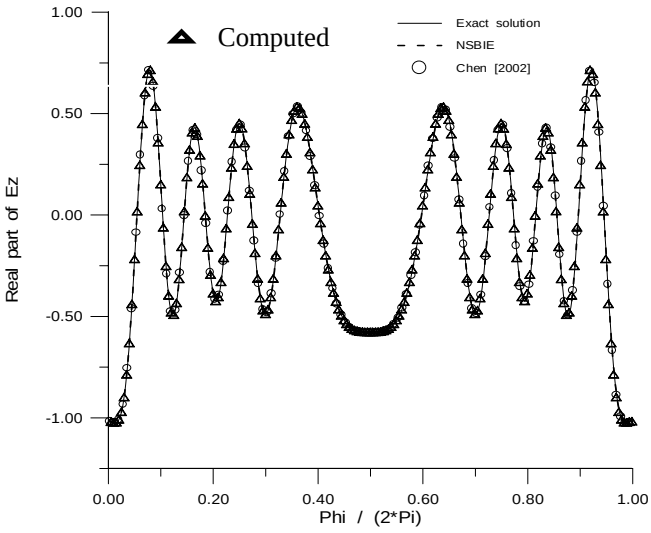

Figure 2 : Re(E_z^s) for a TM^z wave along $r = 4$ by a $a = 2$ perfectly conducting circular cylinder.

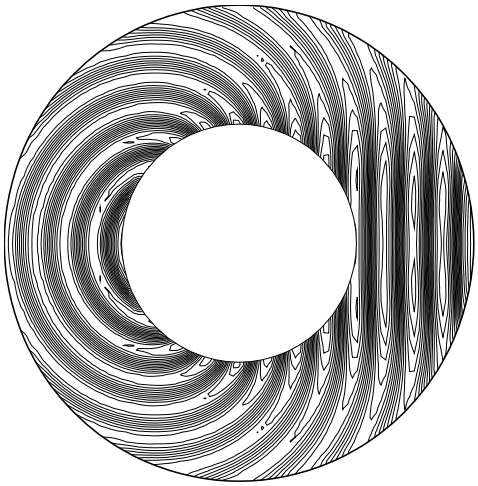

Figure 3 : The contour of Re(E_z^s) for a TM^z wave by a $a = 2$ perfectly conducting circular cylinder.

Table 1 : Computing CPU time of Re(E_z^s) with different numerical methods

elements or node numbers	NSBIE	BEM	MFS
	CPU time	CPU time	CPU time
36	0.11s	0.11s	0.06s
72	0.66s	0.44s	0.14s
144	2.58s	2.03s	0.33s

avoided. The CPU time is defined as the time from the definition of the initial implicit argument to the plot of the scattered electric components along $r = 4$ by a perfectly conducting circular cylinder with $a = 2$. The CPU time is determined for the same PC hardware. Furthermore the contours of the scattered electric field are displayed in Fig. 3 to illustrate the good performance of the MFS simulation.

As far as the far-field boundary contributions of the scattered fields are concerned, the numerical methods of domain approximation have encountered some natural difficulties to circumvent the modeling of the unbounded region. Therefore, several treatments are devoted to overcoming this problem. For illustration, Cecot, Demkowicz and Rachowicz (2000) utilized the finite element/infinite element (FE/IE) to solve the two-dimensional scattering problems. Ledger, Morgan, Hassan and Weatherill (2002) employed the FEM with a perfectly matched layer (PML) and hybrid FEM meshes to get the scattered field of two-dimensional obstacles. And Yao-Bi, Nicolas and Nicolas (1993) have used the FEM and coupling with two methods, boundary element method (BEM) and absorbing boundary conditions (ABC), to solve the unbounded propagation problems. In contrast, the MFS is a meshless numerical method which can treat the unbounded domain very well since the MFS will satisfy the out-going wave exactly. The RCS is obtained as good as Ledger, Morgan, Hassan and Weatherill (2002) did without any special treatment for the far-field boundary. This is due to the far-field property of the fundamental solution that the far-field boundary condition of the physical problem will be automatically satisfied. Besides it is noticed that only 36 source nodes are used in this MFS simulation. Similar procedures are undertaken for the simulation of the scattered fields of the transverse electric (TE^z) wave, as shown in Fig. 1 (a). The distributions of the RCS for the TE^z wave and the TM^z wave are illustrated in Fig. 4 and Fig. 5, respectively. Very accurate results are also obtained from the computation of the MFS as comparing with the results of analytical solution [Harrington (1961)], and FEM simulation [Ledger, Morgan, Hassan and Weatherill (2002)].

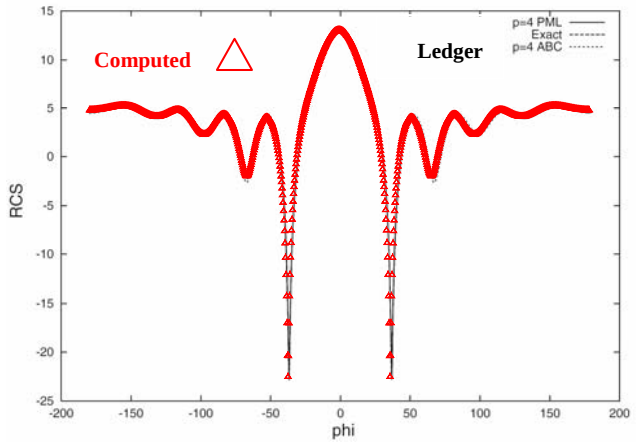

Figure 4 : RCS for a TE^z wave by a $a = 1$ perfectly conducting circular cylinder.

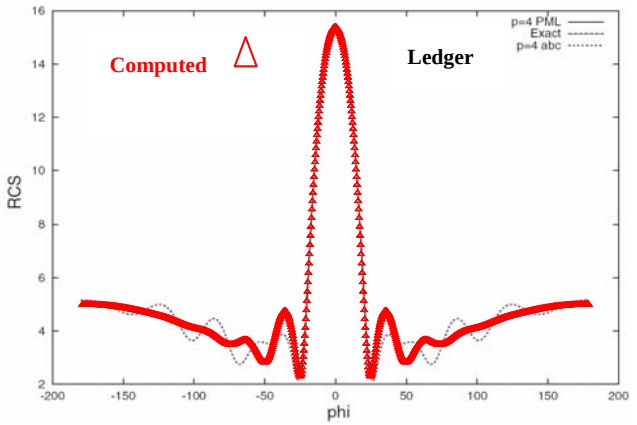

Figure 5 : RCS for a TM^z wave by a $a = 1$ perfectly conducting circular cylinder.

4.2 Scattering By A Conducting Sphere

After the two-dimensional problems have been simulated successfully, the sphere, regarded as a benchmark problem for the three-dimensional computational scattering problems, is the next example to be examined. A uniform plane electric wave, polarized in the x direction with unit amplitude travels along the direction of the positive z axis. The wave is normally incident upon a perfectly conducting sphere of radius a, in the source-free and lossless space as shown in Fig. 6. Similar to the two-dimensional problem, the permittivity, permeability, radius of the sphere and wave length is treated as follows

$$\mu = \varepsilon = 1 \quad \text{and} \quad \lambda = a = 1/2 \tag{21}$$

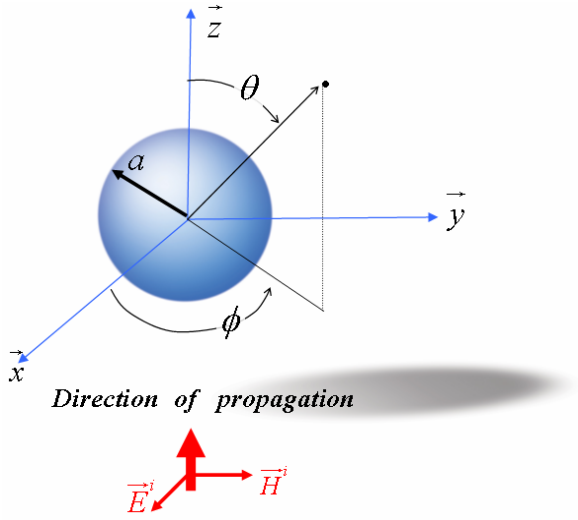

Figure 6 : Normally incident plane wave on a perfectly spherical conductor.

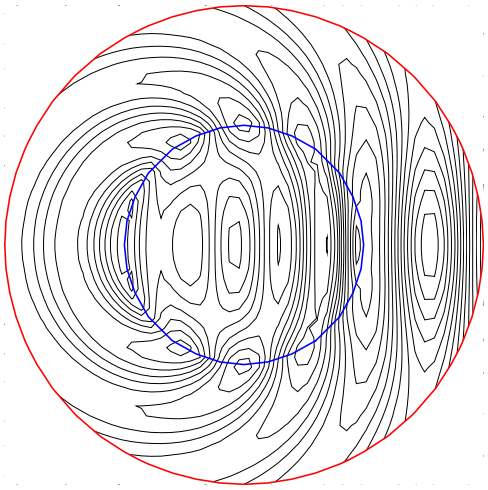

Figure 7 : The contour of Re(E_x^s) on the $x = 0$ plane and surface of the sphere.

The computed contour of the real part of the scattered electric component in the x direction on $x = 0$ plane and the surface of the sphere, shown in Fig. 7, is acceptable by comparing with the FEM result of Morgan, Brookes, Hassan and Weatherill (1998).

As to the far-field problem, present results are displayed in Fig. 8. Excellent results are obtained as compared the RCS profile on the $\phi = \pi/2$ plane with the exact solution [Harrington (1961)] and the conventional BEM [Chen (2002)]. And the comparisons of the RCS on the $\phi = 0$

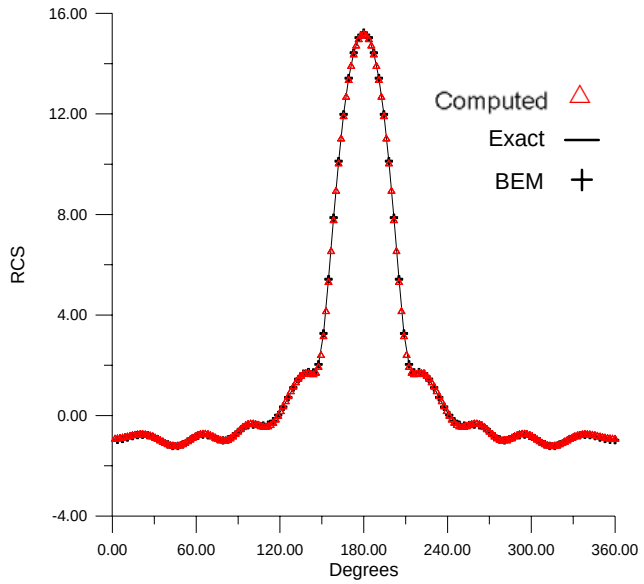

Figure 8 : RCS by a $a = 1/2$ perfectly conducting sphere on the $\phi = \pi/2$ plane

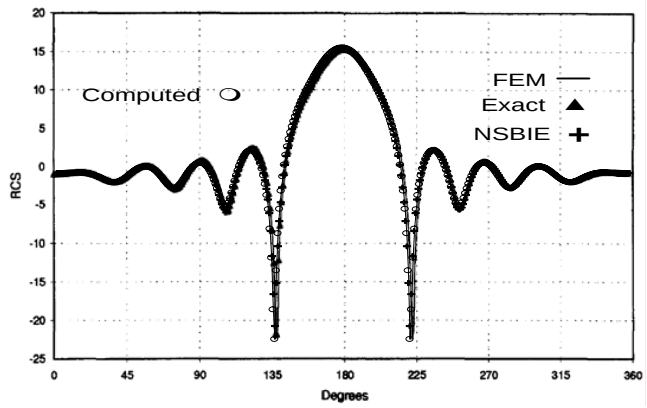

Figure 9 : RCS by a $a = 1/2$ perfectly conducting sphere on the $\phi = 0$ plane

plane with the analytic solution [Harrington (1961)], the NSBIE method [Chiu and Young (2003)] and the FEM [Morgan, Brookes, Hassan and Weatherill (1998)] also reveal the acceptable results, as shown in Fig. 9. It is worthy while to observe that all the above solutions give the same accurate results as compared with the exact solution. However, only 1,344 nodal points are used in the MFS, 3,200 nodal points are employed in both the conventional BEM and NSBIE methods, while 589,505 elements, 706,999 edges and 99,991 nodes are used in the FEM formulation. It is therefore claimed that the MFS is a simple, efficient and accurate numerical scheme in the computational methodology.

4.3 Scattering By A Conducting Prolate Spheroid

In the previous example, the three-dimensional sphere has been successfully formulated. To extend the method to treat the more complex shapes of scatterers, without being limited to just a simple sphere, the scatterers of various geometries can be attempted. Therefore, a prolate spheroid subjected to the same incident wave as the case of the sphere is taken as a final example for modeling the more complicate scatterer as shown in Fig. 10. The three radii of the prolate spheroid are chosen by tak-

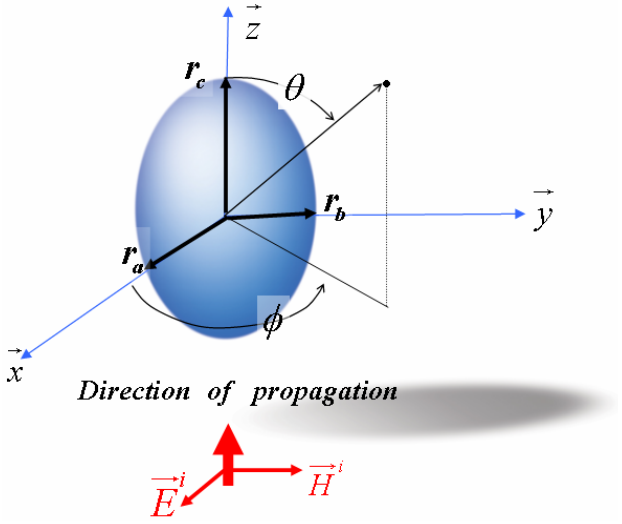

Figure 10 : Normally incident plane wave on a perfectly conducting prolate spheroid.

ing

$$r_a = r_b = 0.5 \quad \text{and} \quad r_c = 0.6 \tag{22}$$

The computed contour of the real part of scattered electric component in the x direction on $x = 0$ plane and the surface of the scatterer is displayed in Fig. 11. The comparisons of results from Fig. 7 and Fig. 11 reveal the rationality of the scattered electric field of the conducting spheroid, when the same wavelength of the incident wave is taken for different geometries. The prolate spheroid accommodates more electric waves than the sphere because of one longer radius. The distributions of the RCS

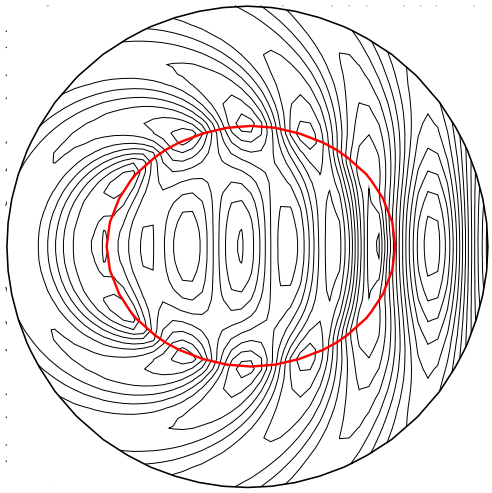

Figure 11 : The contour of Re(E_x^s) on $x = 0$ plane and surface of the prolate spheroid.

on the $\phi = 1/2$ plane and the RCS on $\phi = 0$ plane are shown in Fig. 12 and Fig. 13, respectively. These RCS profiles illustrate the excellent predictive capability of the MFS even for more complex domain with smooth boundary.

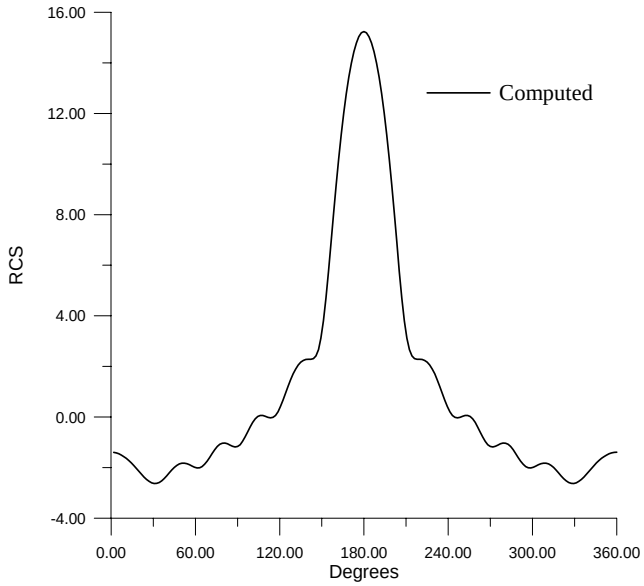

Figure 12 : RCS on the $\phi = 1/2$ plane by a perfectly conducting prolate spheroid.

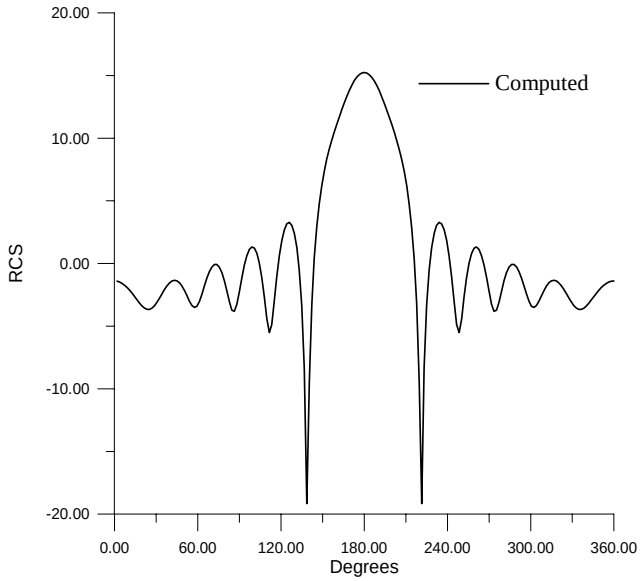

Figure 13 : RCS on the $\phi = 0$ plane by a perfectly conducting prolate spheroid.

5 Conclusion

The innovative MFS for modeling the electromagnetic scattering problems, which are governed by vector Helmholtz equations with coupled boundary conditions, is presented. The distributions of the RCS of a two-dimensional circular conducting cylinder, a three-dimensional conducting sphere, and a three-dimensional prolate spheroid are simulated. Without establishing complex mesh and boundary integration, the MFS, a meshless numerical method, has demonstrated the advantage in the unbounded domain via comparisons with other domain or boundary approximation methods. Moreover, no special treatments are required in the far-field due to the far-field property of the fundamental solutions. The comparisons of the simulated results with the conventional BEM and NSBIE methods have revealed the advantage of the MFS, such as avoiding singular problem and much saving in the CPU time. The MFS also shows the superiority to the FEM in treating the far field boundary of the unbounded domain. The simple, efficient and accurate algorithm of the MFS with fewer nodes than other numerical schemes is confirmed in this presentation. The numerical simulation of the electromagnetic scattering problems by the MFS technique has opened a better approach for the research of the computational electromagnetics.

Acknowledgement: This study is supported by the National Science Council, Taiwan under the grant number NSC 92-2611-E-002-007, it is greatly appreciated. The paper was presented in International Workshop on Mesh-Free Methods [Young and Ruan (2003)]. We would like to express our sincere thanks to Carlos Alves, C. S. Chen and Vitor Leitao for the enthusiastic invitation of our paper in this special issue of meshless methods in the Journal of Computer Modeling in Engineering and Sciences (CMES).

References

Atluri, S. N. (2004): The meshless method (MLPG) for domain & BIE discretizations. 700 pages, *Tech Science Press*.

Atluri, S. N.; Han, Z. D.; Rajendran, A. M. (2004): A new implementation of the meshless finite volume method, through the MLPG "mixed" approach. *CMES: Computer Modeling in Engineering & Sciences*, vol. 6, no. 6, pp. 491-514.

Atluri, S. N.; Shen, S. (2002): The meshless local Petrov-Galerkin (MLPG) method: A simple & less-costly alternative to the finite element and boundary element methods. *CMES: Computer Modeling in Engineering & Sciences*, vol. 3, no. 1, pp. 11-52.

Balanis, C. A. (1982): Antenna theory: analysis and design. *Wiley,* New York.

Cecot, W.; Demkowicz, L.; Rachowicz, W. (2000): A two-dimensional infinite element for Maxwell's equations. *Comput. Methods Appl. Mech. Engrg.*, vol. 188, pp. 625-643.

Chen, C. S.; Golberg, M. A.; Rashed, Y. F. (1998): A mesh-free method for linear diffusion equations. *Numerical Heat Transfer, Part B*, vol. 33, pp. 469-486.

Chen, G. Q. (2002): Application of Helmholtz equation by the boundary element method to the waveguide and scattering propagation problems. *MS Thesis, National Taiwan University*, Taiwan.

Chen W. (2002A): Symmetric boundary knot method. *Engng. Anal. Bound. Elem.,* vol. 26, pp. 489-494.

Chen W. (2002B): Meshfree boundary particle method applied to Helmholtz problems. *Engng. Anal. Bound. Elem.,* vol. 26, pp. 577-581.

Chen W.; Tanaka, M. (2002): A meshless, exponential convergence, integration-free, and boundary-only RBF technique. *Computers and Mathematics with Applications,* vol. 43, pp. 379-391.

Chew, W. C.; Song, J. M.; Cui, T. J.; Velamparambil, S.;Hastriter, M. L.; Hu, B. (2004): Review of large scale computing in electromagnetics with fast integral equation solvers. *CMES: Computer Modeling in Engineering & Sciences*, vol. 5, no. 4, pp. 361-372.

Chiu, C. L.; Young, D. L. (2003): Non-singular boundary integral equation for two-dimensional electromagnetic scattering problems. *The 27th National Conference on Theoretical and Applied Mechanics,* Tainan,Taiwan.

Cho, H. A.; Golberg, M. A.; Muleshkov, A. S.; Li, X. (2004): Trefftz method for time dependent partial differential equations. *Computers, Materials, & Continua*, vol. 1, no.1 , pp. 1-37.

Fairweather, G.; Karageorghis, A. (1998): The method of fundamental solution for elliptic boundary value problems. *Adv. Comput. Math.,* vol. 9, pp. 69-95.

Fairweather, G.; Karageorghis, A.; Martin, P. A. (2003): The method of fundamental solutions for scattering and radiation problems. *Engineering Analysis with Boundary Elements*, vol. 27, pp. 759-769.

Golberg, M. A. (1995): The method of fundamental solutions for Poisson's equation. *Engineering Analysis with Boundary Elements*, vol. 16, pp. 205-213.

Golberg, M. A.; Chen, C. S. (1997): Discrete projection methods for integral equations. *Computational Mechanics Publications*, Southampton.

Harrington, R. F. (1961): Time-harmonic electromagnetic fields. *McGraw-Hill*.

Hassan, O.; Morgan, K.; Jones, J.; Larwood, B.; Weatherill, N. P. (2004): Parallel 3D time domain electromagnetic scattering simulations on unstructured meshes. *CMES: Computer Modeling in Engineering & Sciences*, vol. 5, no. 5, pp. 383-394.

Jingguo, W.; Ahmed, M. T.; Leavers, J. D. (1990): Nonlinear least squares optimization applied to the method of fundamental solutions for eddy current problems. *Transation on Magnetics,* vol. 26, no.5, pp. 2385-2387.

Kupradze, V. D.; Aleksidze, M. A. (1964): The method of functional equations for the approximate solution of certain boundary value problems. *U.S.S.R. Computational Mathematics and Mathematical Physics,* vol. 4, pp. 82-126.

Ledger, P. D.; Morgan, K; Hassan, O.; Weatherill, N. P. (2002): Arbitrary order edge elements for electromagnetic scattering simulations using hybrid meshes and a PML. *Int. J. Numer. Meth. Engng*, vol. 55, pp. 339-358.

Mathon, R.; Johnston R. L. (1977): The approximate solution of elliptic boundary-value problems by fundamental solutions. *SIAM J. Numer. Anal.*, vol. 14, pp. 638-650.

Morgan, K; Brookes, P. J.; Hassan, O.; Weatherill, N. P. (1998): Parallel processing for the simulation of problems involving scattering of electromagnetic waves. *Comput. Methods Appl. Mech. Engrg*, vol. 152, pp. 157-174.

Reitich, F.; Tamma, K. K. (2004): State-of-the-art, trends, and directions in computational electromagnetics. *CMES: Computer Modeling in Engineering & Sciences*, vol. 5, no. 4, pp. 287-294.

Trefftz, E. (1926): Ein gegenstick zum ritzschen vertahven. *Proceedings of 2nd Int. Cong. Appl. Mech., Zurich*, pp. 131-137.

Tsai, C. C.; Young, D. L.; Cheng, A. H.–D. (2002): Meshless BEM for three-dimensional Stokes flows. *CMES: Computer Modeling in Engineering & Sciences*, vol. 3, no.5, pp. 117-128.

Yao-Bi, J. L.; Nicolas, L.; Nicolas, A. (1993): 2D electromagnetic scattering by simple shapes: a quantification of the error due to open boundary. *Transactions on Magnetics*, vol. 29, pp. 1830-1834.

Young, D. L.; Ruan, J. W. (2003): Method of fundamental solutions for modeling electromagnetic wave scattering problems. *International Workshop on Mesh-Free Methods,* July 21-23, 2003, Lisbon, Portugal.